ELSEVIER

www.elsevier.nl/locate/jorganchem

Journal of Organometallic Chemistry 586 (1999) 171–175

Journal of Organometallic Chemistry

Synthesis and crystal structure of a rhodium(III) complex bearing a hypervalent phosphorus(V) ligand as a bidentate ligand and equilibrium between bidentate and monodentate structures in solution

Koichiro Toyota, Yohsuke Yamamoto, Kin-ya Akiba *

Department of Chemistry, Graduate School of Science, Hiroshima University, 1-3-1 Kagamiyama, Higashi-Hiroshima 739-8526, Japan

Received 30 March 1999; received in revised form 7 May 1999

Abstract

A new Rh(III) complex bearing a hypervalent phosphorus(V) ligand, $Rf_2PRh(Cp^*)Cl$ (**4**) (Rf = Martin ligand; *o*-$C_6H_4C(CF_3)_2O$–), was obtained by the reaction of $Rf_2P^-Li^+$ generated in situ with $[Cp^*RhCl_2]_2$. X-ray structural analysis of **4** showed that the hypervalent phosphorus ligand Rf_2P acted as a bidentate ligand coordinating to the Rh center through the phosphorus and one oxygen atom of a Martin ligand. The Rh center became coordinatively saturated and was stabilized by the additional coordination of the oxygen atom. However, in solution the equilibrium between the bidentate (**4A**) and the monodentate (**4B**) species was observed (**4A**:**4B** = 6:1 in C_6H_6, 4:1 in $CHCl_3$, 2:1 in THF, 1.6:1 in CH_2Cl_2), and the monodentate species **4B** became predominant in polar solvents (**4A**:**4B** = 1:2 in CH_3CN, 1:2.5 in CH_3NO_2, 1:3 in DMSO). Therefore, the strong Lewis acidic Rh center can be regarded as masked in the solid state but in solution it becomes unmasked to **4B**, in which a solvent is coordinating to the Rh center.

Keywords: Rhodium complex; Hypervalent phosphorus ligand; Bidentate ligand; Equilibrium

1. Introduction

Compounds bearing a hypervalent Group 15 element–transition metal bond have attracted interest [1–9]. Recently, we were able to prepare and structurally characterize stable several transition metal complexes bearing a hypervalent phosphorus or antimony ligand (**1**) [10,11]. The X-ray structural analysis of these complexes revealed that the phosphoranide or stiboranide ligand acted as a monodentate ligand toward the transition metal atom and the geometry at the P or Sb atom was distorted trigonal bipyramid (TBP) with the transition metal at the equatorial site of the TBP. Here we report synthesis, X-ray structure, and behavior in solution of a new Rh(III) complex bearing a hypervalent phosphorus(V) ligand, $Rf_2PRh(Cp^*)Cl$ (**4**) (Rf = Martin ligand; *o*-$C_6H_4C(CF_3)_2O$–). X-ray structural analysis of this complex showed an interaction between the Rh center and an oxygen atom of a Martin ligand. The interaction can be regarded as an intramolecular Lewis acid–base interaction (structure **4A**). However, in solution the interaction was found to be labile, the equilibrium between the coordinated structure (**4A**) and the uncoordinated structure (**4B**) was observed (Eq. (1)). Although similar interaction has been observed by

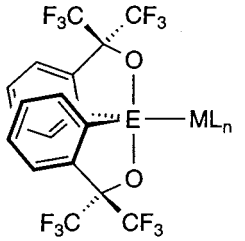

1

E = P, Sb
M = Cr, Mo, W, Fe, Ru, Ni, Pd
L_n = $Cp(CO)_2$, dppe, etc.

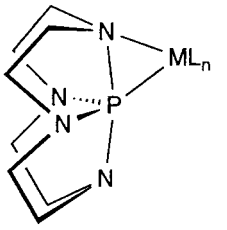

2

M = Mo, L_n = $Cp(CO)_2$
M = Pt, L_n = PPh_3, Cl

* Corresponding author. Tel.: +81-824-24-7430; fax: +81-824-24-0723.

E-mail address: akiba@sci.hiroshima-u.ac.jp (K.-y. Akiba)

0022-328X/99/$ - see front matter
PII: S0022-328X(99)00259-4

Riess's or Lattman's group for **2** in the solid state [6–9], this is the first observation for the equilibrium between monodentate and bidentate species in solution for compounds having a hypervalent Group 15 element–transition metal bond. It is interesting to note that in **4B** the Lewis acidic Rh center can be regarded as unmasked. The equilibrium ratios in various solvents were examined and in polar solvents **4B** was found to be predominant over **4A**.

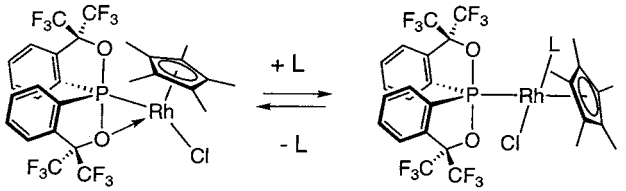

4A L: solvent or Me_3P **4B**

2. Experimental

2.1. Materials and apparatus

All reactions were carried out under dry Ar using Schlenk techniques. THF was freshly distilled from sodium–benzophenone and CH_2Cl_2 was freshly distilled from CaH_2 under dry N_2. All other liquid reagents were also distilled from CaH_2 under dry N_2. The preparation of $[Cp^*RhCl_2]_2$ [12,13] and Rf_2PH [14] followed published procedures. Melting point was taken on a Yanagimoto micro melting point apparatus and is uncorrected. ^{1}H-NMR (400 MHz), ^{19}F-NMR (376 MHz) and ^{31}P-NMR (162 MHz) spectra were recorded on a Jeol EX-400 spectrometer. Chemical shifts are reported (δ scale) from internal Me_4Si for ^{1}H, from external $CFCl_3$ for ^{19}F, or from external 85% H_3PO_4 for ^{31}P. Elemental analysis was performed on a Perkin–Elmer 2400 CHN elemental analyzer.

2.2. Synthesis of $Rf_2PRh(Cp^*)Cl$ (4)

$[Rf_2P]^-Li^+$ was generated by treatment of Rf_2PH (**3**, 206 mg, 0.40 mmol) with *t*-BuLi (1.64 M in *n*-pentane, 0.24 ml, 0.40 mmol) in THF (5 ml) at -78°C for 15 min. $[Cp^*RhCl_2]_2$ (136 mg, 0.22 mmol) dissolved in 10 ml of CH_2Cl_2 was added to the solution. The mixture was stirred for 15 h at room temperature (r.t.) and was filtered. After all volatile compounds were removed, the product was extracted with *n*-hexane. Complex **4** (291 mg, 0.37 mmol) was obtained in 92% yield as a reddish-brown powder in a pure form after *n*-hexane was removed. m.p. ca. 205°C (dec.). ^{1}H-NMR ($CDCl_3$) **4A**: δ 1.64 (d, 15H, $J_{Rh-H} = 4.4$ Hz), 7.1 ~ 8.5 (m, 8H); **4B**: δ 1.36 (d, 15H, $J_{Rh-H} = 4.4$ Hz), 7.1 ~ 8.5 (m, 8H). ^{19}F-NMR ($CDCl_3$) **4A**: δ -75.5 (q, 3F, $J_{F-F} = 10$ Hz), -74.8 (q, 3F, $J_{F-F} = 10$ Hz), -74.6 (q, 3F, $J_{F-F} = 4$ Hz), -73.3 (q, 3F, $J_{F-F} = 4$ Hz); **4B**: δ -75.2 (q, 3F, $J_{F-F} = 10$ Hz), -73.7 (q, 3F, $J_{F-F} = 10$ Hz), -73.3 (q, 3F, $J_{F-F} = 10$ Hz), -72.8 (q, 3F, $J_{F-F} = 10$ Hz). ^{31}P-NMR ($CDCl_3$) δ 17.3 (d, $J_{Rh-P} = 169$ Hz, **4B**), 190.9 (d, $J_{Rh-P} = 221$ Hz, **4A**); (C_6H_6) δ 16.2 (d, $J_{Rh-P} = 180$ Hz, **4B**), 191.8 (d, $J_{Rh-P} = 221$ Hz, **4A**); (CH_2Cl_2) δ 17.2 (d, $J_{Rh-P} = 180$ Hz, **4B**), 190.8 (d, $J_{Rh-P} = 224$ Hz, **4A**); (THF) δ 15.7 (d, $J_{Rh-P} = 184$ Hz, **4B**), 191.7 (d, $J_{Rh-P} = 224$ Hz, **4A**); (CH_3CN) δ 6.8 (d, $J_{Rh-P} = 188$ Hz, **4B**), 192.1 (d, $J_{Rh-P} = 224$ Hz, **4A**); (CH_3NO_2) δ 17.7 (d, $J_{Rh-P} = 186$ Hz, **4B**), 192.9 (d, $J_{Rh-P} = 227$ Hz, **4A**); (DMSO) δ 12.4 (d, $J_{Rh-P} = 188$ Hz, **4B**), 192.1 (d, $J_{Rh-P} = 228$ Hz, **4A**). Anal. Calc. for $C_{28}H_{23}ClF_{12}O_2PRh$: C, 42.64; H, 2.94. Found: C, 42.93; H, 2.75.

2.3. Crystal Structure of 4

Crystal data and numerical details of the structure determinations are given in Table 1. Data for **4** were collected on a Mac Science DIP2030 imaging plate equipped with graphite-monochromated Mo–K_α radiation ($\lambda = 0.71073$ Å). Unit cell parameters were determined by autoindexing several images in each data set separately with program DENZO [15]. From the cell constants and systematic absences, the space group was chosen to be $P2_1/a$. For each data set, rotation images were collected in 3° increments with a total rotation of

Table 1
Crystal data for **4**

Empirical formula	$C_{28}H_{23}O_2ClF_{12}PRh$
Molecular weight	788.81
Crystal system	Monoclinic
Space group	$P2_1/a$
Crystal dimensions (mm)	$0.20 \times 0.15 \times 0.08$
a (Å)	16.9470(7)
b (Å)	11.2380(4)
c (Å)	17.5110(8)
α (°)	90
β (°)	116.265(2)
γ (°)	90
V (Å^3)	2990.8(1)
Z	4
D_{calc} (g cm^{-3})	1.530
Absorption coefficient (cm^{-1})	0.8028
$F(000)$	1568
Radiation, λ (Å)	Mo–K_α; 0.710 73
Temperature (K)	298
Data collected	$+h$, $+k$, $\pm l$
Total data collected, unique, observed	7177, 6689, 5675 [$I > 3\sigma(I)$]
No. of parameters refined	406
R, R_w, S	0.065, 0.073, 4.540
Max shift in final cycle	0.0327
Final difference map, max (e Å^{-3})	0.44

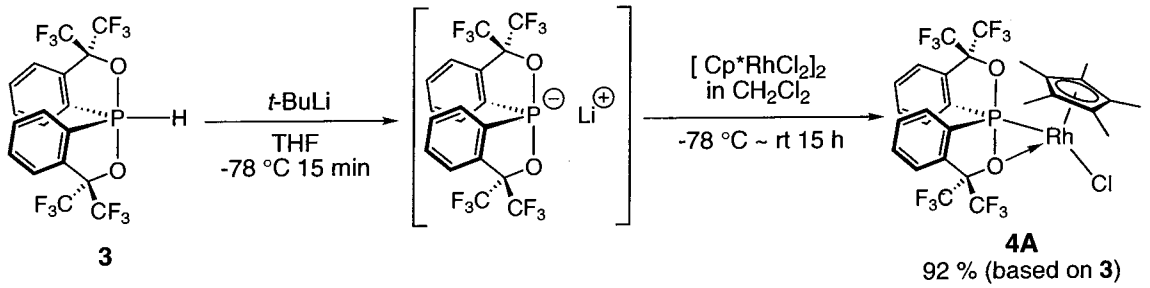

Scheme 1.

180° about ϕ. Data were processed by using SCALEPACK [15]. The structures were solved by a direct method with the program CRYSTAN-GM (Mac Science) and refined by full-matrix least squares. All non-hydrogen atoms were refined with anisotropic thermal parameters. No absorption correction was applied. All hydrogen atoms could be found on a difference Fourier map; these coordinates were included in the refinement with isotropic thermal parameters.

3. Results and discussion

First of all, we attempted to synthesize Rh(I) complexes bearing a hypervalent phosphorus(V) ligand by the reaction of several Rh(I) halide complexes with lithium phosphoranide, $Rf_2P^-Li^+$, generated in situ from the reaction of Rf_2PH (**3**) with *t*-BuLi at -78°C. When $RhCl(PPh_3)_3$, $RhCl(CO)(PPh_3)_2$, or $[RhCl(cod)]_2$ with 1,3-bis(diphenylphosphino)propane were used as Rh sources, any desirable products were not obtained. In the case of $RhCl(cod)(PPh_3)$, $Rf_2PRh(cod)(PPh_3)$ was observed quantitatively based on the ^{31}P-NMR spectrum {δ 7.4 (dd, $J_{Rh-P} = 178$ Hz, $J_{P-P} = 50$ Hz) and 23.5 (dd, $J_{Rh-P} = 160$ Hz, $J_{P-P} = 50$ Hz} of the reaction mixture, but the product was too unstable to isolate. In contrast, stable Rh(III) complex $Rf_2PRh(Cp^*)Cl$ (**4**) was obtained in 92% yield by the reaction of $[Cp^*RhCl_2]_2$ in CH_2Cl_2 with $Rf_2P^-Li^+$ generated in situ in THF at -78°C (Scheme 1). Complex **4** was stable to oxygen and atomospheric moisture in the solid state, but it was decomposed by hydrolysis and heating in solution. **4** was characterized by ^{1}H-, ^{19}F-, ^{31}P-NMR, elemental analysis, and X-ray structural analysis.

Suitable crystals (reddish-brown plate) of **4** for X-ray structural analysis were obtained by recrystallization from *n*-hexane at room temperature. Fig. 1 shows the ORTEP drawing (30% probability ellipsoids) of **4**. Selected bond lengths and bond angles are listed in Table 2. The O1–P1–O2, and C1–P1–C10 bond angles are 178.9(1)° and 121.5(1)°, respectively, therefore the geometry around the phosphorus(V) atom can be considered as trigonal bipyramid (TBP). The equatorial Cp*RhCl fragment is coordinated by both the phosphorus (Rh–P bond length: 2.276(1) Å) and one oxygen atom (Rh–O2 bond length: 2.502(2) Å) of a Martin ligand to form a three membered ring and is located between the apical P1–O2 bond (structure **4A**). The P1–O2 bond length (1.916(2) Å) is elongated by 0.166 Å than the P1–O1 bond length (1.750(2) Å). The coordination of the oxygen atom of a Martin ligand stablizes the Rh center which becomes coordinatively saturated. Similar coordination of transition metals (Mo and Pt) has been observed by Riess's or Lattman's group for **2** but the coordination was with the nitrogen instead of the oxygen [6–9]. However, in our Martin ligand system, this is the first observation of such coordination because the oxygen atom of a Martin ligand has been inert due to the electron-withdrawing effect and the steric bulkiness of the two CF_3 groups based on our experience on the synthesis of various

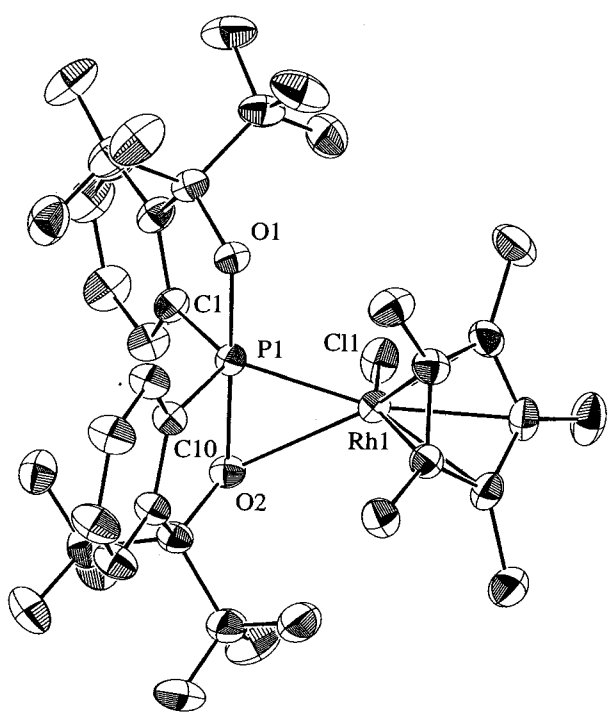

Fig. 1. ORTEP drawing (30% probability ellipsoids) of **4**.

Table 2
Selected bond lengths (Å) and bond angles (°) of **4**

Bond lengths (Å)		Bond angles (°)	
Rh1–Cl1	2.353(1)	P1–Rh1–O2	47.0(1)
Rh1–P1	2.276(1)	Rh1–O2–P1	60.3(1)
Rh1–O2	2.502(2)	Rh1–P1–O1	108.0(1)
Rh1–C19	2.098(3)	Rh1–P1–O2	72.7(1)
Rh1–C20	2.242(2)	Rh1–P1–C1	122.7(1)
Rh1–C21	2.270(2)	Rh1–P1–C10	112.0(1)
Rh1–C22	2.190(2)	O1–P1–O2	178.9(1)
Rh1–C23	2.162(2)	O1–P1–C1	88.3(1)
P1–O1	1.750(2)	O1–P1–C10	93.9(1)
P1–O2	1.916(2)	O2–P1–C1	91.9(1)
P1–C1	1.826(2)	O2–P1–C10	85.1(1)
P1–C10	1.834(2)	C1–P1–C10	121.5(1)

transition metal complexes bearing a hypervalent Group 15 element ligand [10,11]. Therefore, it can be concluded that the Rh center has much stronger Lewis acidity than several transition metals examined (**1**).

In solution, ^{31}P-NMR spectrum of **4** at ambient temperature (293 K) shows two signals at δ 190.9 (d, $J_{Rh-P} = 221$ Hz) and 17.3 (d, $J_{Rh-P} = 169$ Hz) in the ratio of 4:1 in $CDCl_3$. Since both signals show large Rh–P couplings and the ratio changes to 1.6 (δ 190.8): 1 (δ 17.2) in CH_2Cl_2, it can be concluded that there is an equilibrium between two species bearing a Rh–P bond and the equilibrium is attained within a few minutes. The ^{31}P-NMR chemical shifts of the major species at very low fields (δ 190.9 in $CDCl_3$, 190.8 in CH_2Cl_2) suggest that one of the P–O bond is elongated and is weakened by the additional coordination of the Rh atom with the oxygen atom resulting in a partial phosphine–metal bond. Similar observations have been reported for HcyclenPMo(CO)$_5$ [16] and Hcyclen-Rh(Cp)Cl [17]. Therefore, the major species is consistent with the bidentate structure (**4A**). The ^{31}P-NMR chemical shifts (δ 17.3 in $CDCl_3$, 17.2 in CH_2Cl_2) of the minor species are comparable to the reported values in $Rf_2PFeCp(CO)_2$ (δ 14.7 in $CDCl_3$) [2] and $Rf_2PPd(dppe)(Cl)$ (δ 4.6 in $CDCl_3$) [11] in which the monodentate structures were confirmed by X-ray analysis. Therefore, the minor species can be assigned to the monodentate structure (**4B**) together with the major species as the bidentate structure (**4A**) (Eq. (1)). The assignment is consistent with the result of the equilibrium ratio in various solvents. That is, although the equilibrium is shifted toward **4A** in less polar solvents {**4A**:**4B** = 6 (δ 191.8): 1 (δ 16.2) in C_6H_6; 4 (δ 190.9): 1 (δ 17.3) in $CHCl_3$; 2 (δ 191.7): 1 (δ 15.7) in THF; 1.6 (δ 190.8): 1 (δ 17.2) in CH_2Cl_2}, the ratio of the equilibrium is reversed and **4B** becomes the major component in more polar solvents {**4A**:**4B** = 1 (δ 192.1): 2 (δ 6.8) in CH_3CN; 1 (δ 192.9): 2.5 (δ 17.7) in CH_3NO_2; 1 (δ 192.1): 3 (δ 12.4) in DMSO}. The polar solvent would coordinate to the Rh center instead of an oxygen atom of a Martin ligand as shown in Eq. (1). By addition of two equivalents of Me_3P to the THF solution of the equiliblium mixture, the low field signal (**4A**) disappeared and only high field signals {δ 4.5 (dd, $J_{Rh-P} = 221$ Hz, $J_{P-P} = 66$ Hz) and -0.6 (dd, $J_{Rh-P} = 169$ Hz, $J_{P-P} = 66$ Hz} were obserevd. The species should be monodentate **4B** with Me_3P coordinating to the Rh center based on the chemical shift and the large P–P coupling through Rh. The P–P coupling ($J_{P-P} = 66$ Hz) corresponds to *cis* P–Rh–P configuration because more than 200 Hz of J_{P-P} is typically observed for *trans* P–Rh–P configuration [18]. To our knowldge the equilibrium between monodentate and bidentate structures in solution is the first example for compounds having a hypervalent Group 15 element–transition metal bond although similar bidentate coordination was observed for **2** in the solid state [6–9]. In **4** the strong Lewis acidic Rh center can be regarded as masked in the solid state (**4A**) and in solution it becomes unmasked to **4B**, in which a solvent is coordinating to the Rh center.

4. Supplementary material

Atomic coordinates, bond lengths and angles, and thermal parameters of **4** have been deposited at the Cambridge Crystallographic Data Centre, CCDC No. 127419. Copies of this information may be obtained free of charge from The Director, CCDC, 12 Union Road, Cambridge, CB2 1EZ, UK (Fax: +44-1223-336-033; e-mail: deposit@ccdc.cam.ac.uk or www: http://www.ccdc.cam.ac.uk). See Information for Authors, Issue No. 1. Any request to the CCDC for this material should quote the full literature citation and the reference number.

Acknowledgements

The authors would like to thank Central Glass Co. for supplying us with 1,1-bis(trifluoromethyl)benzyl alcohol. Part of this work was supported by a Grant-in-Aid for Scientific Research on Priority Areas (A), 'The Chemistry of Inter-element Linkage' (No. 09239103) from the Ministry of Education, Science, Sports, and Culture, Japan.

References

[1] K. Kubo, H. Nakazawa, T. Mizuta, K. Miyoshi, Organometallics 17 (1998) 3522.
[2] S.K. Chopra, J.C. Martin, Heteroat. Chem. 2 (1991) 71.
[3] R. Faw, C.D. Montgomery, S.J. Rettig, B. Shurmer, Inorg. Chem. 37 (1998) 4136.
[4] W. Malisch, P.H. Panster, Angew. Chem. Int. Ed. Engl. 13 (1974) 670.

[5] W. Malisch, H.-A. Kaul, E. Gross, U. Thewalt, Angew. Chem. Int. Ed. Engl. 21 (1982) 549.
[6] J. Wachter, B.F. Mentzen, J.G. Riess, Angew. Chem. Int. Ed. Engl. 20 (1981) 284.
[7] J.-M. Dupart, A. Grand, S. Pace, J.G. Riess, J. Am. Chem. Soc. 104 (1982) 2316.
[8] M. Lattman, S.K. Chopra, A.H. Cowley, A.M. Arif, Organometallics 5 (1986) 677.
[9] M. Lattman, E.G. Burns, S.K. Chopra, A.H. Cowley, A.M. Arif, Inorg. Chem. 26 (1987) 1926.
[10] Y. Yamamoto, M. Okazaki, Y. Wakisaka, K.-y. Akiba, Organometallics 14 (1995) 3364.
[11] K. Toyota, Y. Yamamoto, K.-y. Akiba, J. Chem. Res. (S), in press.
[12] J.W. Kang, P.M. Maitlis, J. Am. Chem. Soc. 91 (1969) 5970.
[13] C. White, A. Yates, P.M. Maitlis, Inorg. Synth. 29 (1992) 228.
[14] I. Granoth, J.C. Martin, J. Am. Chem. Soc. 101 (1979) 4623.
[15] Z. Otwinowski, University of Texas, Southwestern Medical Center. The program is available from Mac Science Co.
[16] D.V. Khasnis, M. Lattman, U. Siriwardane, Organometallics 10 (1991) 1326.
[17] E.G. Baurns, S.S.C. Chu, P. de Meester, M. Lattman, Organometallics 5 (1986) 2383.
[18] S. Berger, S. Brain, H.-O. Kalinowski (Eds.), NMR Spectroscopy of the Non-metallic Elements, Wiley, New York, 1997, p. 960.